

Supporting Information for

Temperature effects in Dye-Sensitized Solar Cells

*Sonia R. Raga, Francisco Fabregat-Santiago**

Photovoltaic and Optoelectronic Devices Group, Departament de Física, Universitat Jaume I, 12071
Castelló, Spain

Email: fabresan@fca.uji.es

Measuring performance stability of DSC for 500h.

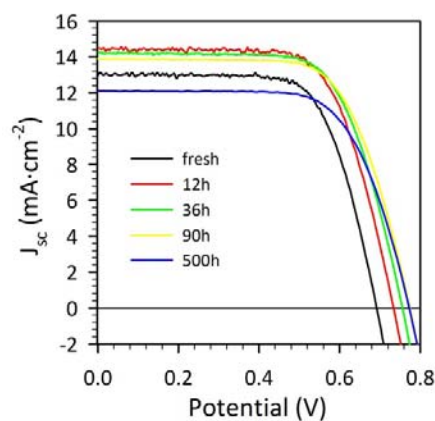


Figure S1. *J-V* curves performed to the average of a batch of 5 dye solar cells in a lapse of 500h after cell assembly. Samples were measured at 1 sun with class A solar simulator.

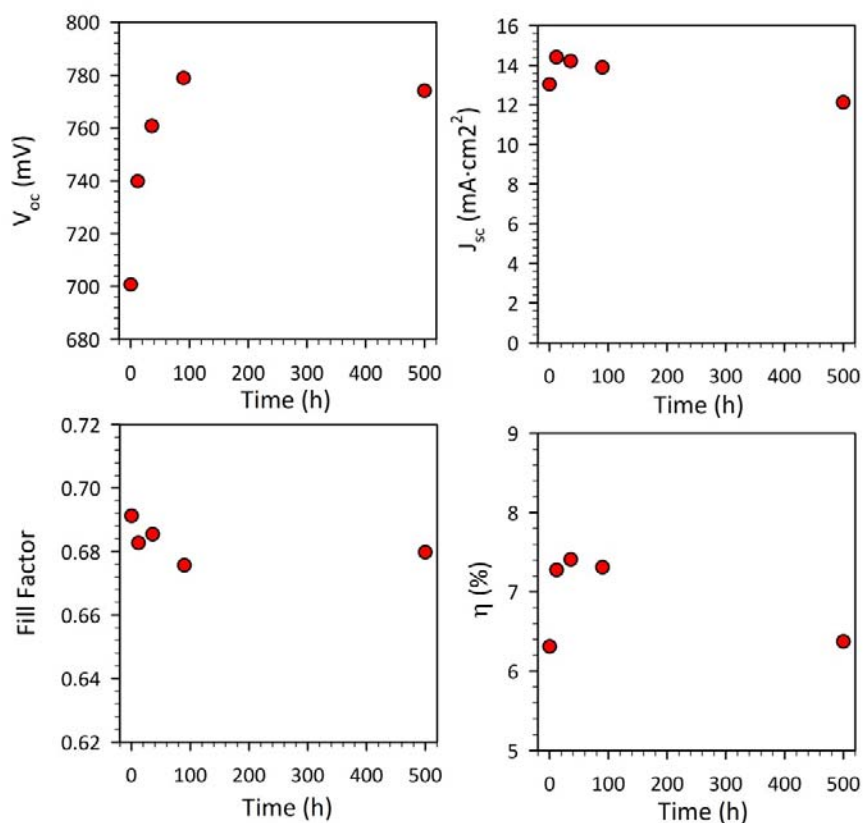


Figure S2. Evolution of average performance parameters for 5 dye solar cells with time. Maximum in efficiency is reached after 4 days from cell assembly, then J_{sc} and V_{oc} decreases until it reaches a nearly constant value where the cell stabilizes with a smooth decay after 21 days. Performance parameters were obtained under 1 sun illumination provided by a solar simulator.

Impedance of DSC's at different conditions

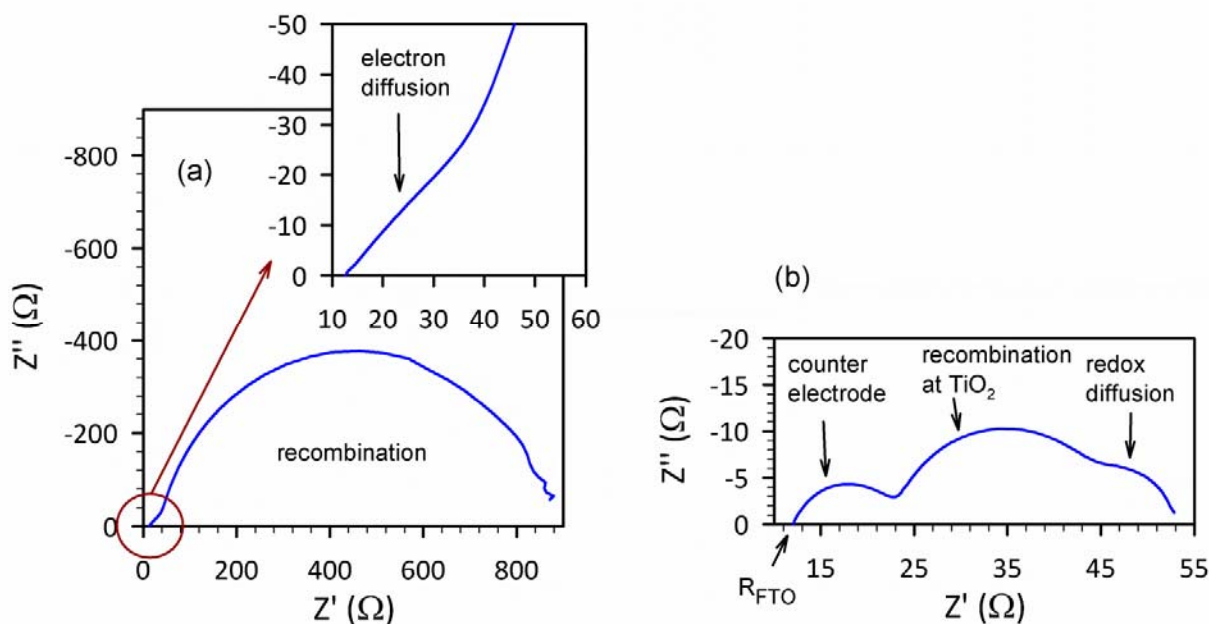


Figure S3. Characteristic trends found for the impedance spectra of samples at different conditions: (a) at middle potentials (here 0.5V, for a cell at 50°C and in the dark) the characteristic spectra of a transmission line with recombination appears. At high frequency, a straight line of slope ~ 1 which origin is the diffusion of electrons in the TiO_2 . At low frequency, an arc accounting for charge recombination and chemical capacitance of TiO_2 . Diffusion impedance is confused with this second arc and may not be distinguished. (b) at potentials around and above V_{oc} (here 0.9V for a cell at -7°C and under illumination), three arcs displaced from the origin by the amount R_{FTO} are observed. The first is associated to the counter electrode charge transfer and capacitance, the second to chemical capacitance and charge recombination at the surface of TiO_2 and the third to the redox species diffusion. Note that diffusion and recombination are partially overlapped. This is attributed to the use of methoxypropionitrile as solvent.

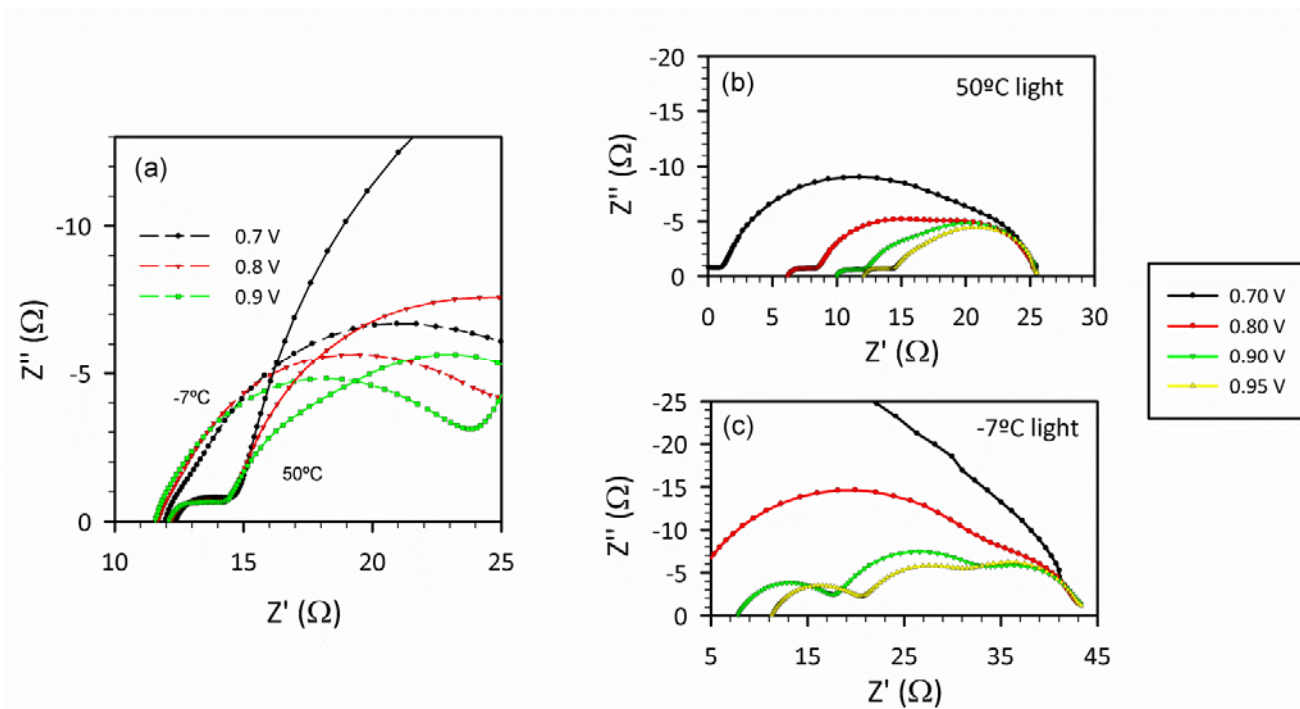


Figure S4. Evolution of impedance spectra with potential at different temperatures. In (a) the values and changes of R_{FTO} and R_{Pt} may be observed at both -7°C and 50° under illumination. In (b) and (c) all the spectra have been shifted to for a better comparison of the diffusion arc at the different potentials.

Values of conduction band shift and plotting capacitance values front V_{ecb} .

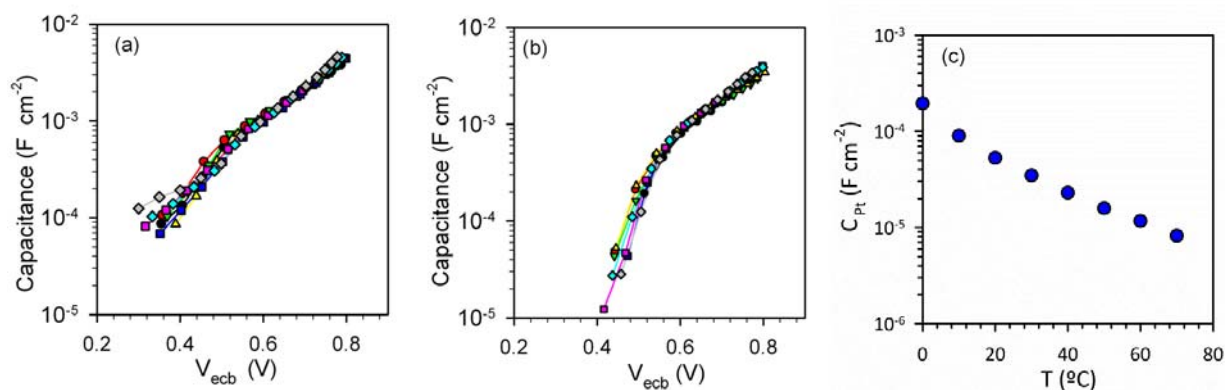


Figure S5. Capacitance data from Figures 4(a) and 4(b) plotted at V_{ecb} in the dark (a) and under illumination (b). The ΔE_c applied to obtain V_{ecb} is detailed in Table S2. (c) Variation of platinumized FTO counter electrode capacitance at different temperatures.

T (°C)	$\Delta E_c/q$ (mV) dark	$\Delta E_c/q$ (mV) light
-7	Ref.	-5
-2	2	-3
3	14	-3
10	34	17
20	47	40
30	61	60
40	80	83
50	87	95
60	96	102
70	109	110

Table S1. Conduction band shift calculated from Eq. 4 and taking as reference the value of E_c at -7°C in the dark.

Comparing capacitance in dark and illumination conditions.

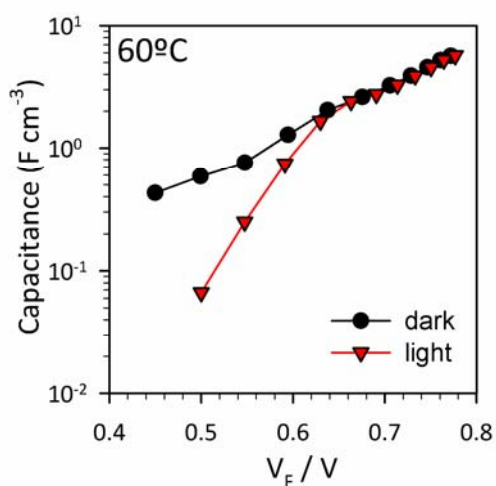


Figure S6. Comparison between TiO_2 capacitance in dark (black dots) and illumination conditions (red triangles). Chemical capacitance at the higher potentials overlaps for both illumination conditions. The peak observed at 0.55V in dark condition changes into a capacitance decay at low potentials under illumination.

Transport resistance

Transport resistance corroborates the results found for capacitance measurements. Transport resistance follows

$$R_{tr} = R_{tr0} \exp\left[\frac{E_c - E_{Fn}}{k_B T}\right] \quad (\text{S1})$$

where E_c is the energy of the conduction band edge, E_{Fn} the Fermi level of electrons, R_{tr0} a constant indicating transport resistance when $E_{Fn} = E_c$, k_B Boltzmann constant and T the absolute temperature.

In Figure S7(a) we observe that R_{tr} decreases with the measurements taken at increasing temperature. For the dark measurements (lines) the slope of R_{tr} diminishes at higher temperature as derived from Eq. (S1) while data under illumination (dots) seem to have in general a lower slope than in the dark, suggesting an increase in temperature of the TiO₂ film as corroborated by R_{rec} measurements shown in the text. A part of this change of slope, at the same temperatures, transport resistance both in the dark and under illumination present nearly the same values as expected. According to Eq. (S1) the changes observed for the different measurements are related to variations in E_c .

If the E_c shift obtained from capacitance data is used to study the variations of transport resistance with T , we obtain the Figure S7(b) with R_{tr} represented vs. the potential at the common equivalent conduction band position. The differences of data in the dark (lines) now become minimal, only differentiated by the slope. Data under illumination, dots in Figure S7(b), collapse within the experimental error (5-15%), in common values and slope as consequence of the films having similar temperatures.

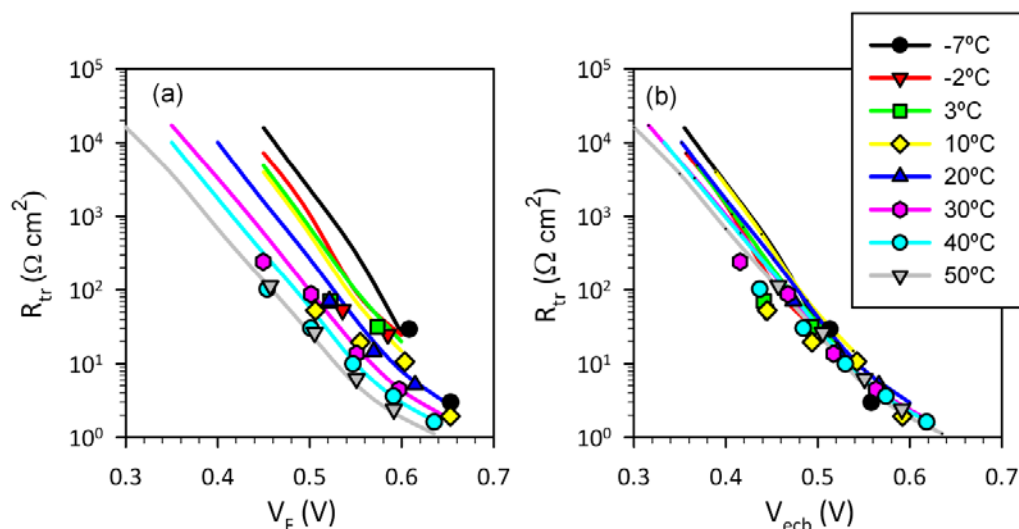


Figure S7. Values of TiO₂ transport resistances in dark (lines) and illumination conditions (dots) versus corrected potential (a) and versus equivalent conduction band potential (b).

Note that using the common representation of R_{tr} vs the applied potential, Figure S8, it is possible to think that light conditions affect TiO₂ conductivity, by increasing it. However, the adequate representation of R_{tr} versus the corrected potential V_F , clarifies this aspect as shown in Figure S7.

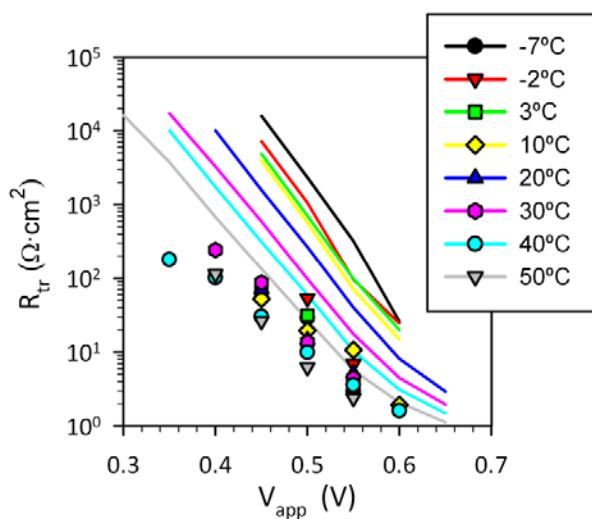


Figure S8. Representation of R_{tr} in the dark (lines) and under illumination (dots) at the different temperatures vs. the applied potential. Apparent differences between data in dark and under illumination are due to series resistance drop.

T (°C)	J_{sc} (mA·cm ⁻²)	V'_{oc} (V)	FF'	η'_{app} (%)
-7	10.3	0.81	0.60	5.03
-2	10.3	0.81	0.61	5.10
3	10.3	0.82	0.61	5.22
10	10.3	0.82	0.63	5.29
20	10.3	0.81	0.63	5.28
30	10.3	0.82	0.65	5.47
40	10.3	0.81	0.66	5.48
50	10.3	0.77	0.69	5.49
60	10.3	0.75	0.70	5.40
70	10.3	0.73	0.71	5.34

Table S2. Characteristic parameters determining the efficiency of DSC with the potentials shifted ΔE_c as shown in Figure 5(b).